

Supplementary Materials for
Distinct roles of ORAI1 in T cell–mediated allergic airway inflammation and immunity to influenza A virus infection

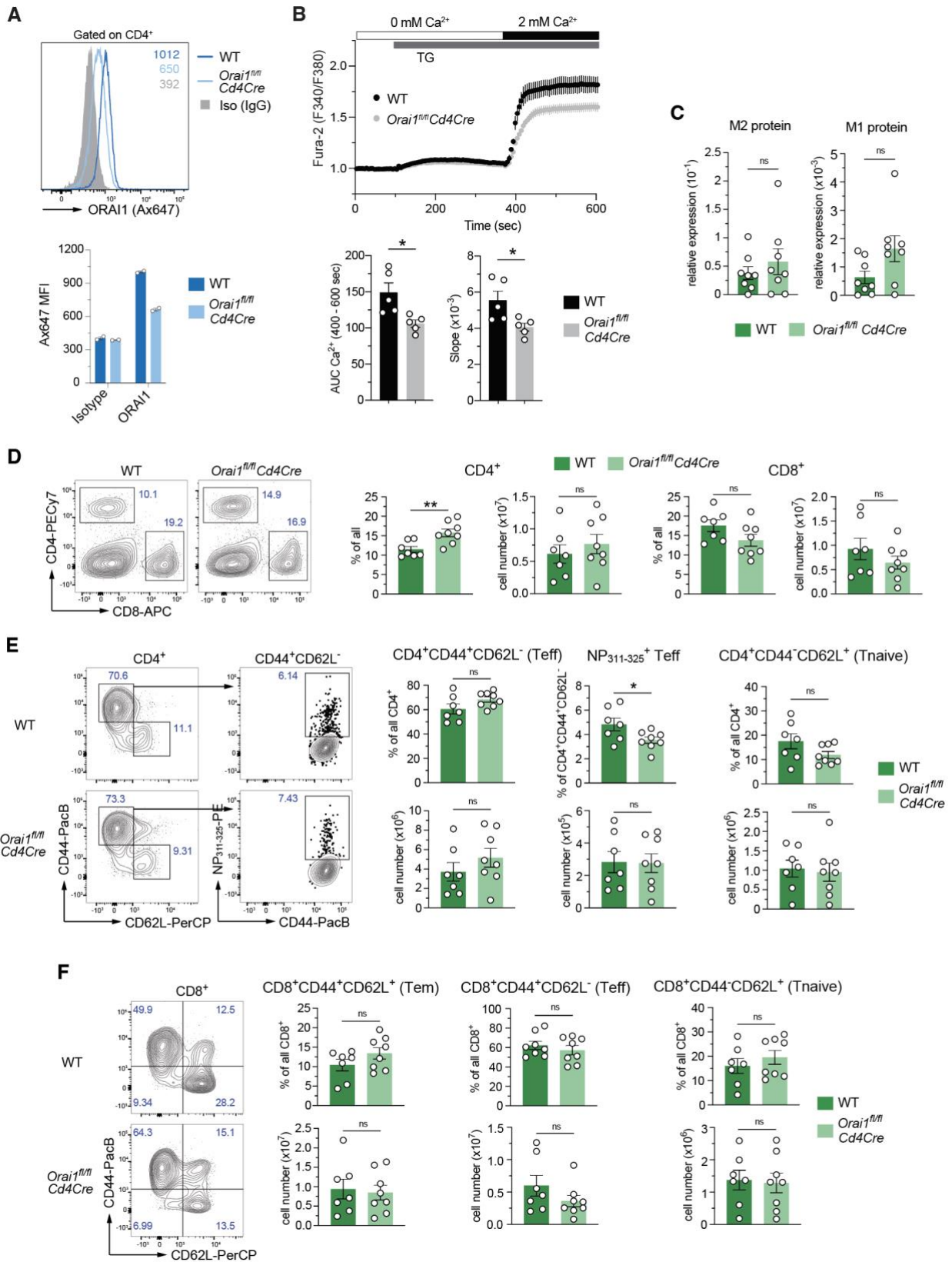
Yin-Hu Wang *et al.*

Corresponding author: Stefan Feske, feskes01@nyumc.org

Sci. Adv. **8**, eabn6552 (2022)
DOI: 10.1126/sciadv.abn6552

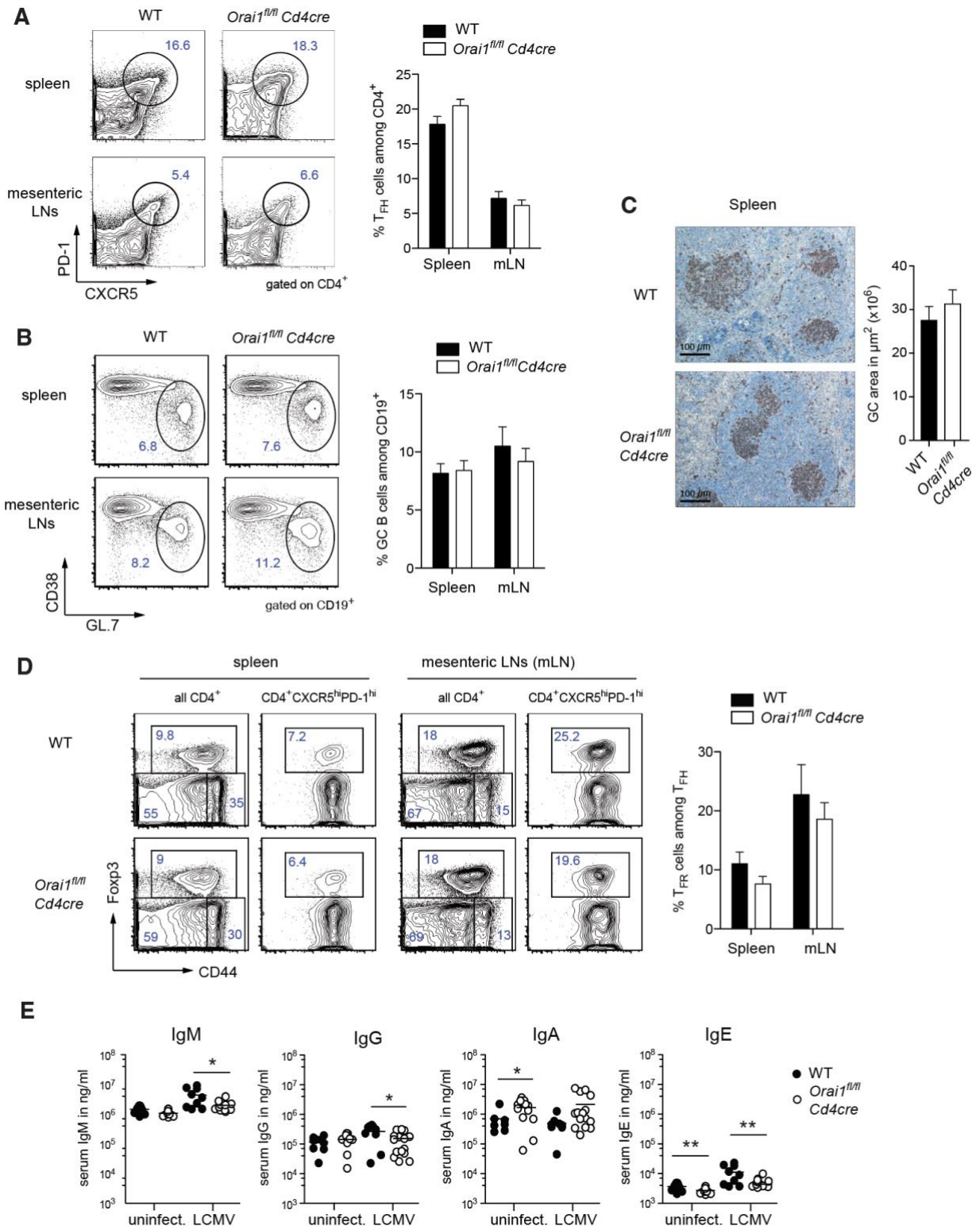
This PDF file includes:

Figs. S1 to S10
Tables S1 to S3



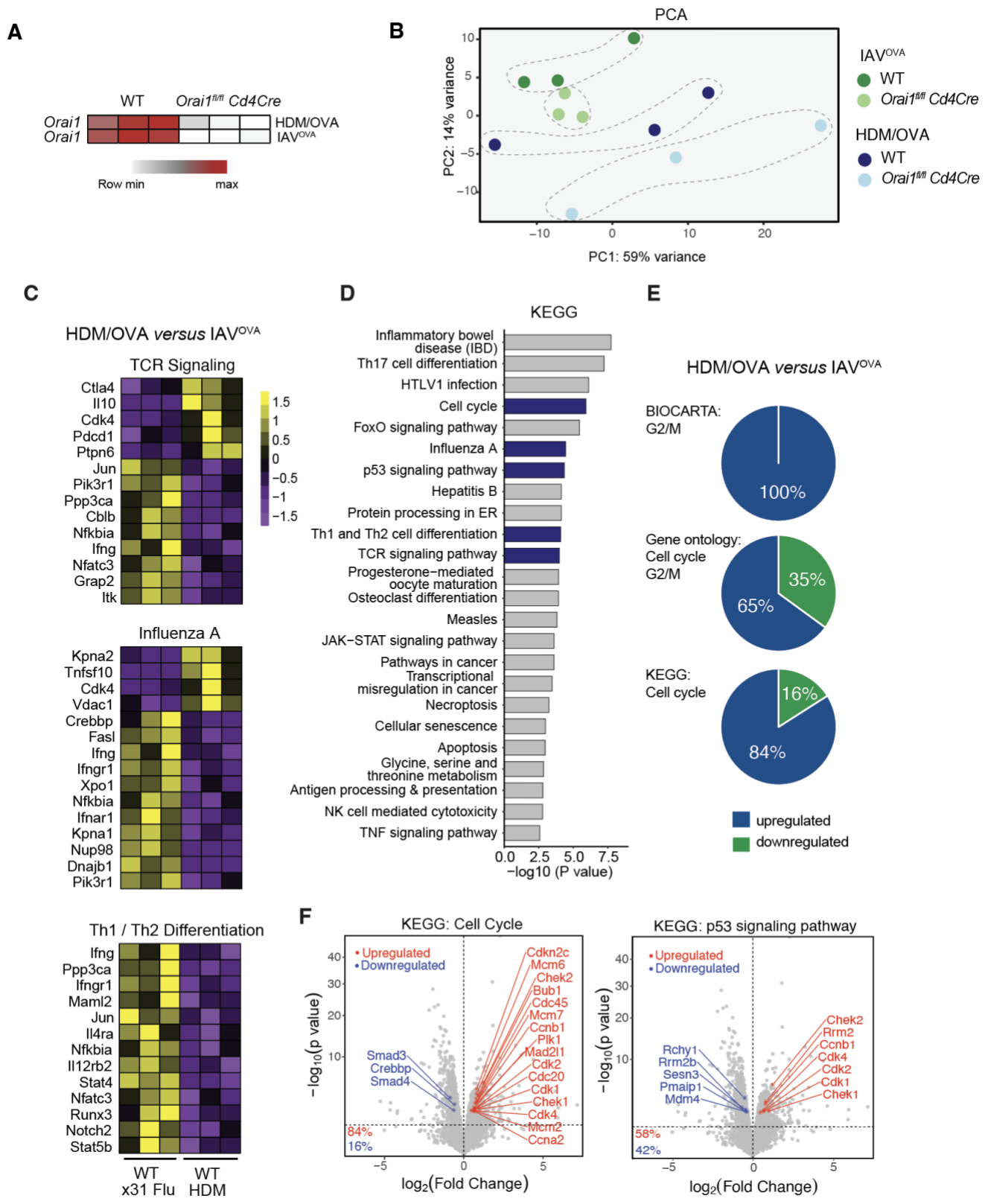
Supplementary Figure 1. Intact T cell mediated Ca immune response to influenza A virus infection in mice with T cell-specific deletion of *Orai1*. **A**, Representative flow cytometry plots and quantification of ORAI1 protein levels in *in vitro* differentiated Th2 cells from WT and *Orai1^{fl/fl}Cd4Cre* mice. Cell were

incubated with affinity-purified rabbit-anti-human ORAI1 antibody or rabbit IgG as isotype (iso) control. Data are representative of two repeat experiments. **B**, Cytosolic Ca^{2+} levels in naïve CD4^+ T cells isolated from the spleen of WT and *Orai1^{fl/fl}Cd4Cre* mice. T cells were loaded with Fura-2 and stimulated with 1 μM thapsigargin (TG) in Ca^{2+} free Ringer solution, followed by perfusion with 2 mM extracellular Ca^{2+} . Quantification of the area under the curve (AUC) and the slope of Ca^{2+} influx after Ca^{2+} readdition. Data are the mean \pm SEM from 5 mice per genotype, pooled from 3 independent experiments. **C**, qRT-PCR analysis of IAV levels in total lung tissue from WT versus *Orai1^{fl/fl}Cd4Cre* mice at day 9 after infection with the x31 (H3N2) strain of influenza A virus (IAV). M2 and M1 proteins represent different genomic regions of IAV. **D**, Representative flow cytometry plots, frequencies and total numbers of CD4^+ and CD8^+ T cells in the lungs of WT and *Orai1^{fl/fl}Cd4Cre* mice 9 days after IAV infection. **E**, Representative flow cytometry plots, frequencies and numbers of total and IAV-specific (NP311-325 tetramer positive) $\text{CD44}^+\text{CD62L}^-$ effector (Teff) and $\text{CD44}^-\text{CD62L}^+$ naïve (Tnaive) CD4^+ T cells in lungs of WT and *Orai1^{fl/fl}Cd4Cre* mice at day 9 after IAV infection. **F**, Representative flow cytometry plots, frequencies and numbers of $\text{CD44}^+\text{CD62L}^+$ effector memory (Tem), $\text{CD44}^+\text{CD62L}^-$ effector (Teff) and $\text{CD44}^-\text{CD62L}^+$ naïve (Tnaive) CD8^+ T cells in lungs of WT and *Orai1^{fl/fl}Cd4Cre* mice at day 9 after IAV infection. Data in C are the mean \pm SEM of 8 mice per cohort from 2 independent experiments. Data in D, E, F are the mean \pm SEM from 7-8 mice per cohort from 2 independent experiments. Statistical analysis by paired (A) or unpaired (C-F) Student's t-test with the following significance levels: *** $p < 0.001$ ** $p < 0.01$ * $p < 0.05$. ns, not significant.



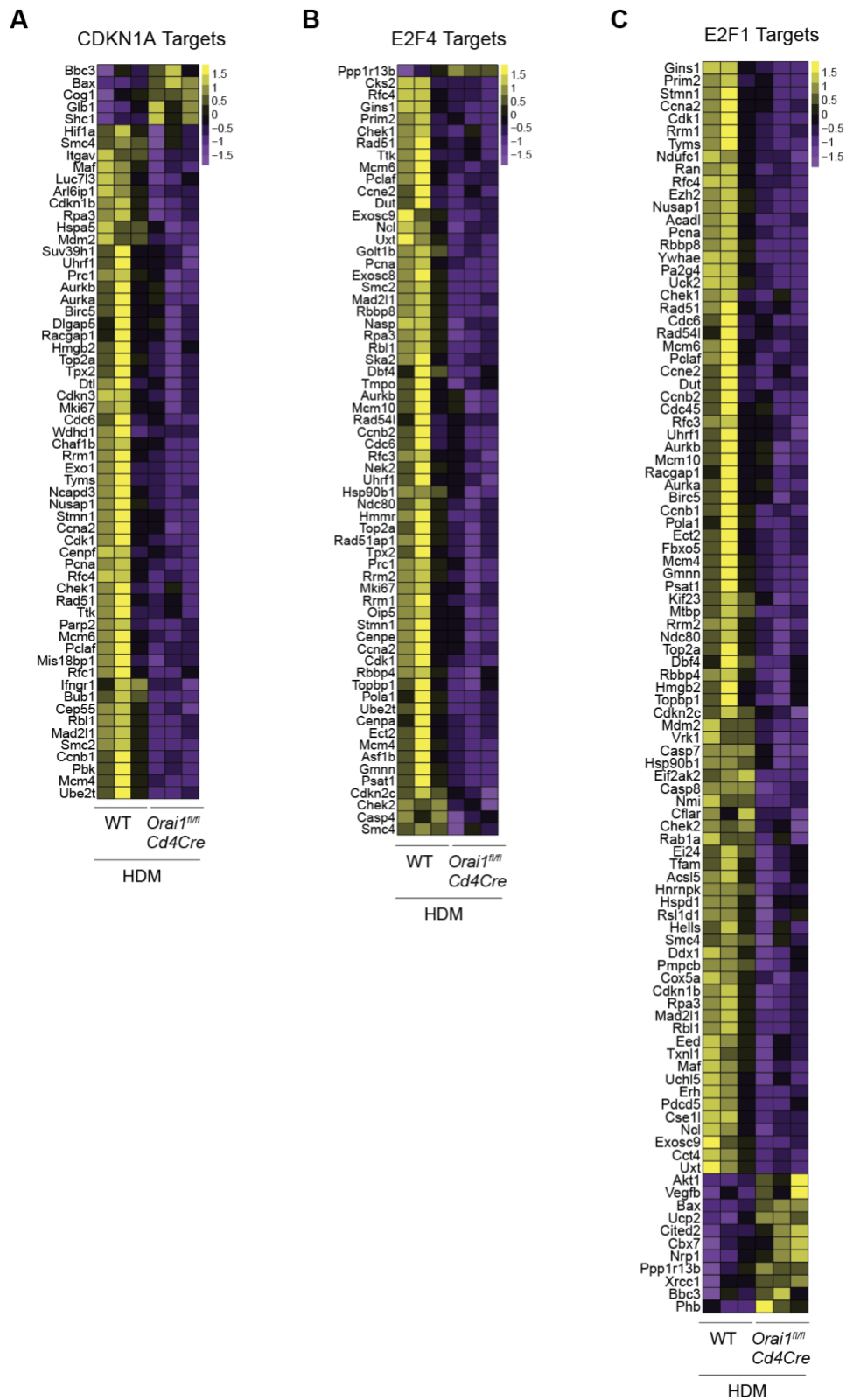
Supplementary Figure 2. T cell-specific deletion of *Orai1* does not impair adaptive immune responses to infection with lymphocytic choriomeningitis virus (LCMV). **A**, Frequencies of CD4⁺PD-1^{hi}CXCR5^{hi} T follicular helper (T_{FH}) cells in the spleens and mesenteric LNs (mLNs) of WT and *Orai1^{fl/fl}Cd4Cre* mice 10 days after infection with the Armstrong strain of LCMV. Data represent the mean ± SEM of 12-18 mice per group. **B**, Frequencies of CD19⁺CD38⁺GL-7⁺ germinal center (GC) B cells in the spleens and mLNs of WT and *Orai1^{fl/fl}Cd4Cre* mice at day 10 p.i. Data are the mean ± SEM of 16-23 mice

per group. **C**, Representative immunohistochemistry staining for peanut agglutinin (PNA) of the spleens of WT and *Orai1^{fl/fl}Cd4Cre* mice 10 days after LCMV infection. **D**, Frequencies of CD4⁺PD-1^{hi}CXCR5^{hi}CD44^{hi}FoxP3⁺ T follicular regulatory (Tfr) cells in the spleens and mLN of WT and *Orai1^{fl/fl}Cd4Cre* mice at day 10 p.i. Data are the mean \pm SEM of 12-16 mice per group. **E**, Total serum levels of IgM, IgG, IgA and IgE in WT and *Orai1^{fl/fl}Cd4Cre* mice before and 10 days after LCMV infection. Data are the mean \pm SEM of 7-15 individual serum samples. Statistical analysis by unpaired Student's t-test with the following significance levels: * p <0.05, ** p <0.01.

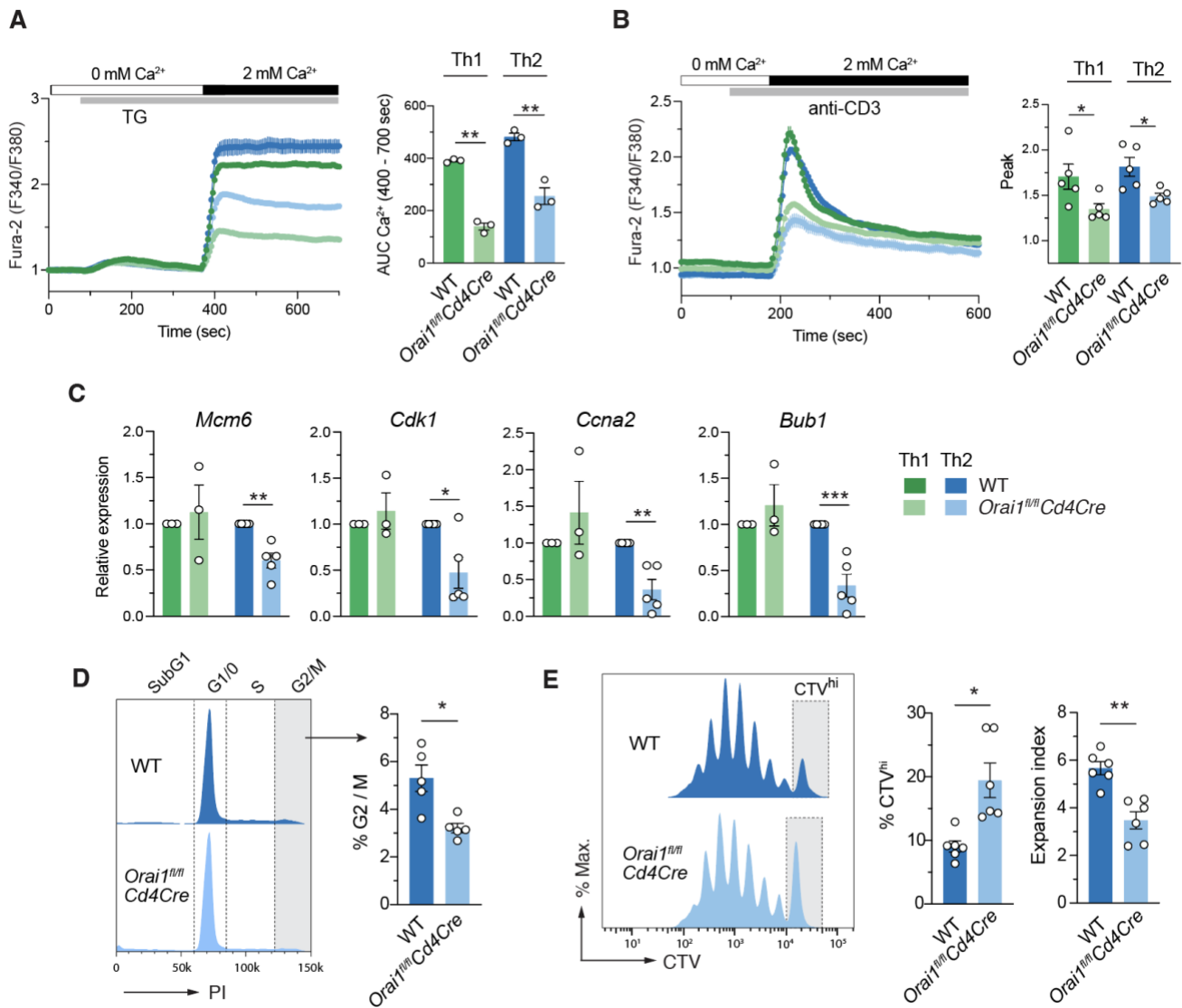


Supplementary Figure 3. ORAI1 regulates differential expression of cell cycle-associated genes in CD4⁺ T cells after induction of allergic airway inflammation by HDM/OVA. A-B, RNA-Seq analysis of differentially expressed genes (DEG) in CD4⁺ T cells of WT OT-II and *Orai1^{fl/fl} Cd4Cre* OT-II donor mice in

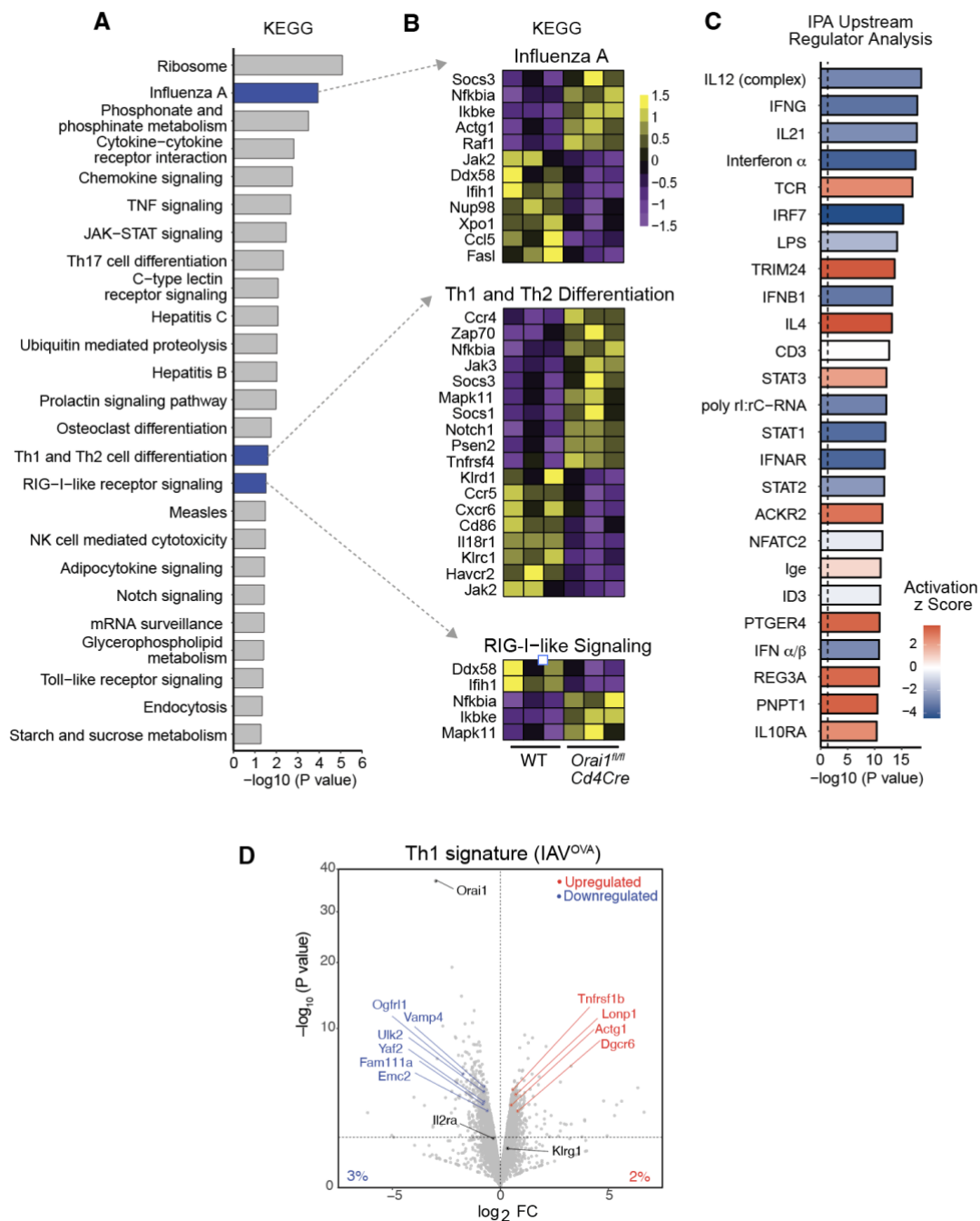
response to HDM/OVA immunization and IAV^{OVA} infection. The experimental designs are shown in Figure 3A,B. **A**, Heatmap showing normalized *Orai1* mRNA expression in CD4⁺ T cells after HDM/OVA immunization or IAV^{OVA} infection. **B**, Principal component analysis (PCA) of the indicated groups. **C**, Heatmaps comparing expression of genes contained in the KEGG pathways *TCR signaling*, *Influenza A* and *Th1/Th2 Differentiation* in WT OT-II T cells after IAV^{OVA} infection and HDM/OVA treatment. **D**, Differentially regulated KEGG pathways in OT-II T cells from IAV^{OVA} infected and HDM/OVA treated mice ranked by the $-\log_{10}$ of *p* values. Statistical analysis by Fisher's exact test: $p < 0.1$. **E**, Percentage of up- and downregulated genes in the BIOCARTA pathway *Cell cycle G2M Checkpoint*, the Gene ontology pathway *Cell cycle G2/M* and the KEGG pathway *Cell cycle* in OT-II T cells from IAV^{OVA} infected and HDM/OVA treated mice. **F**, Differentially expressed genes (DEG) in OT-II T cells from IAV^{OVA} infected and HDM/OVA treated mice. DEG belonging to the KEGG pathways *Cell cycle* and *p53 signaling* that are up- and downregulated are indicated in red and blue, respectively. Data are from WT OT-II and *Orai1^{fl/fl}Cd4Cre* OT-II donor T cells isolated from 3 IAV^{OVA}-infected and 3 HDM/OVA-treated TCR $\alpha^{-/-}$ mice. Statistical analysis in D and F by Fisher's exact test using a *p* value cut-off < 0.1 .



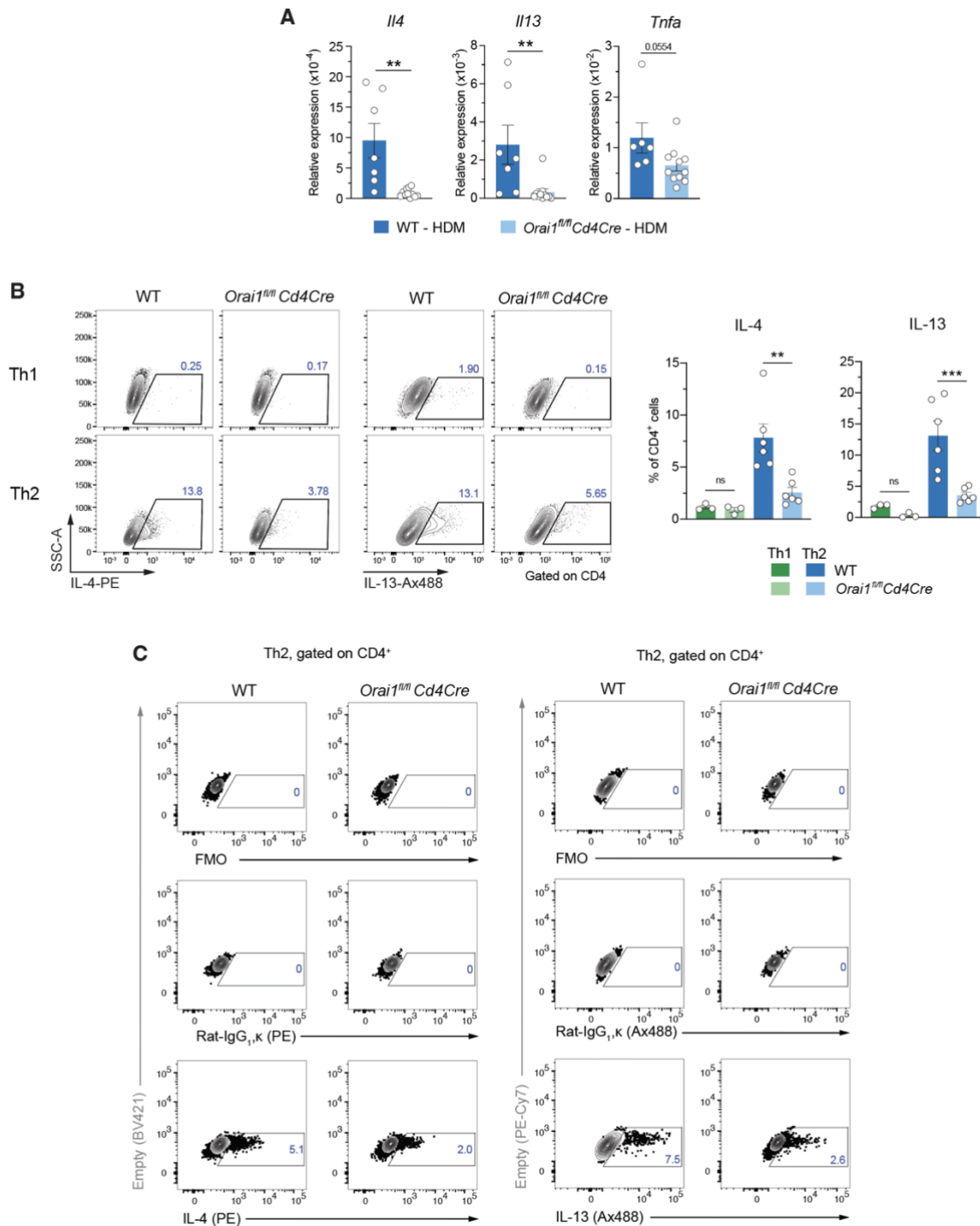
Supplementary Figure 4. ORAI1 regulates differential expression of targets genes of the cell cycle-regulators CDKN1A, E2F4 and E2F1 in pulmonary CD4⁺ T cells after immunization with HDM/OVA. RNA-Seq data are from the same experiment described in Supplementary Fig.4. Heatmaps of DEG regulated by CDKN1A (A), E2F4 (B) and E2F1 (C) in WT and *Orai1*-deficient CD4⁺ T cells after HDM/OVA immunization. Colors represent the Z score expression relative to average expression per row.



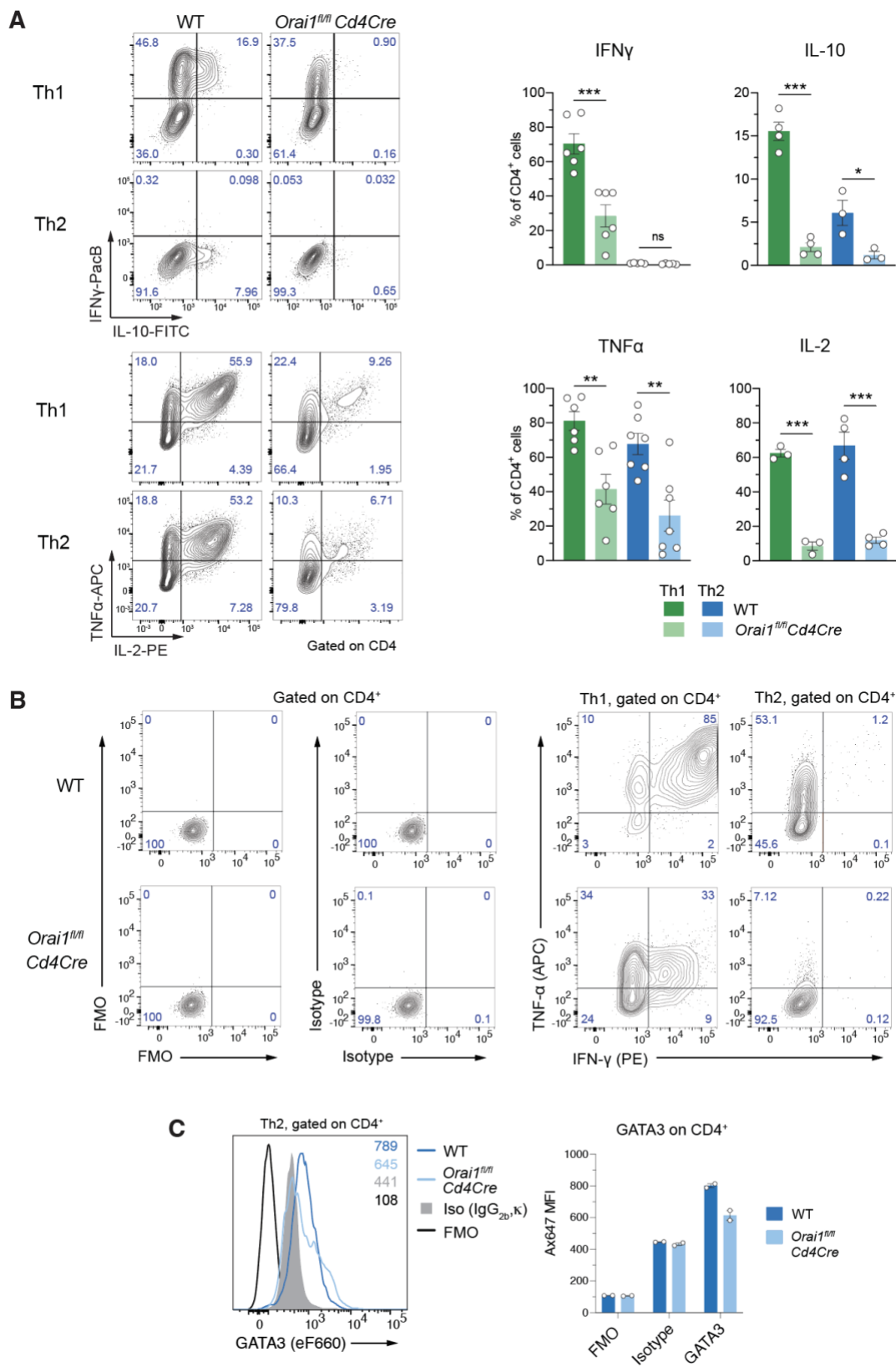
Supplementary Figure 5. ORAI1 regulates the expression of cell cycle-regulating genes and the proliferation of Th2 cells. **A-B**, Cytosolic Ca²⁺ levels in Th1 and Th2 cells derived from CD4⁺ T cells of WT and *Orai1^{fl/fl}*Cd4Cre mice. T cells were loaded with Fura-2 and stimulated with 1 μM thapsigargin (TG) (**A**) or anti-CD3 crosslinking (**B**) in Ca²⁺ free Ringer solution, followed by readdition of 2 mM extracellular Ca²⁺. Quantification of the area under the curve (AUC, in **A**) or peak (**B**) following Ca²⁺ readdition. **C**, Cell cycle-regulating genes identified by RNA-Seq were analyzed for mRNA levels by qRT-PCR in Th1 and Th2 cells of WT and *Orai1^{fl/fl}*Cd4Cre mice at day 5 of *in vitro* polarization. Expression levels were normalized to *Rpl32* house keeping gene and WT T cells. **D**, Cell cycle analysis of WT and *Orai1^{fl/fl}*Cd4Cre mice 3 days following stimulation with anti-CD3 and anti-CD28 dynabeads (T cell : dynabead ratio of 1:4) in the presence of IL-4 and anti-IFN γ . Cells were stained with propidium iodide on day 3 post-stimulation. **E**, Proliferation of Th2 cells of WT and *Orai1^{fl/fl}*Cd4Cre mice following stimulation as in (C). T cells were loaded with CellTrace Violet (CTV) and analyzed at day 4 post-stimulation. Data in A-E are the mean \pm SEM from 3-6 mice per genotype, pooled from 3-4 independent experiments. Statistical analysis by paired (A,B,D,E) or unpaired (C) Student's t-test with the following significance levels: *** p <0.001 ** p <0.01 * p <0.05.



Supplementary Figure 6. Dysregulated gene expression and signaling pathways in *Orai1*-deficient T cells after IAV infection. Analysis of differentially expressed genes (DEG) and pathways in WT OT-II and *Orai1^{fl/fl} Cd4Cre* OT-II donor CD4⁺ T cells isolated from TCR $\alpha^{-/-}$ recipient mice following IAV^{OVA} infection. The experimental design is shown in Figure 3A. **A**, KEGG pathway analysis comparing WT and *Orai1*-deficient T cells. Shown are the top 25 deregulated pathways ranked by p value. **B**, Heatmaps of DEG included in the KEGG pathways *Influenza A*, *Th1/Th2 Differentiation* and *RIG-I-like Signaling* shown in (A). **C**, IPA Upstream Regulator Analysis of DEG in WT OT-II and *Orai1^{fl/fl} Cd4Cre* OT-II CD4⁺ T cells after IAV^{OVA} infection. Upstream regulators are ranked by p value. Colors indicate the activation Z score. **D**, Volcano plot of DEG (in gray) in WT OT-II and *Orai1^{fl/fl} Cd4Cre* OT-II CD4⁺ T cells following infection with IAV^{OVA}. DEG belonging to the Th1 signature *Th1 vs naive CD4 Tcell up* (M3376) published in (76) that are upregulated in *Orai1*-deficient T cells are indicated in red; downregulated DEG are shown in blue. Data in A-D are from 3 IAV^{OVA} infected mice per cohort. Statistical analysis in A and C by Fisher's exact test using a p value cut-off < 0.1.

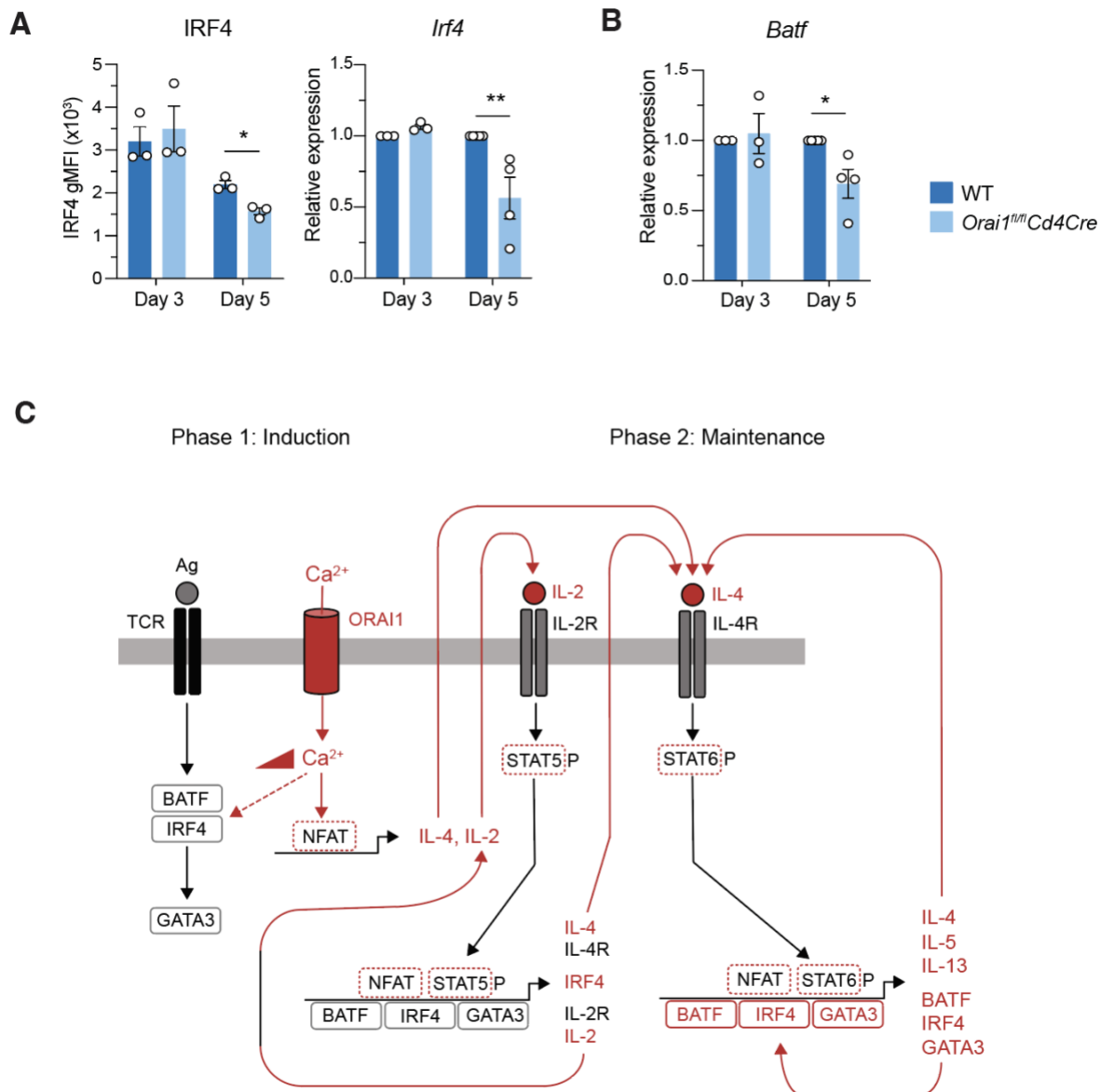


Supplementary Figure 7. ORAI1 is required for the production of cytokines by Th2 cells *in vitro* and *in vivo*. **A**, Expression of cytokine genes in whole lung tissue of WT and *Orai1^{fl/fl}*Cd4Cre mice after HDM challenge analyzed by qRT-PCR. **B**, Representative flow cytometry plots and frequencies of intracellular IL-4 and IL-13 cytokine staining in CD4⁺ T cells of WT and *Orai1^{fl/fl}*Cd4Cre mice that were polarized into Th1 and Th2 cells *in vitro* and analyzed after 5 days and stimulation with PMA/ionomycin for 4h. **C**, Representative flow cytometry plots of IL-4 and IL-13 production by CD4⁺ T cells from WT and *Orai1^{fl/fl}*Cd4Cre mice that were differentiated into Th2 cells for 5 days *in vitro* and stimulated with PMA/ionomycin for 4h. The isotype control antibodies are rat IgG_{1,κ} conjugated with PE or Ax488. Fluorescence minus one (FMO) was determined by staining with anti-CD4 (APC-Cy7), and LIVE/DEAD™ Fixable Blue Dead Cell Stain without either anti-IL-4 or anti-IL-13. Data are the mean ± SEM of 3-6 mice per genotype from at least 3 independent experiments. Statistical analysis by unpaired Student's t-test with the following significance levels: ****p* < 0.001; ***p* < 0.01; **p* < 0.05.

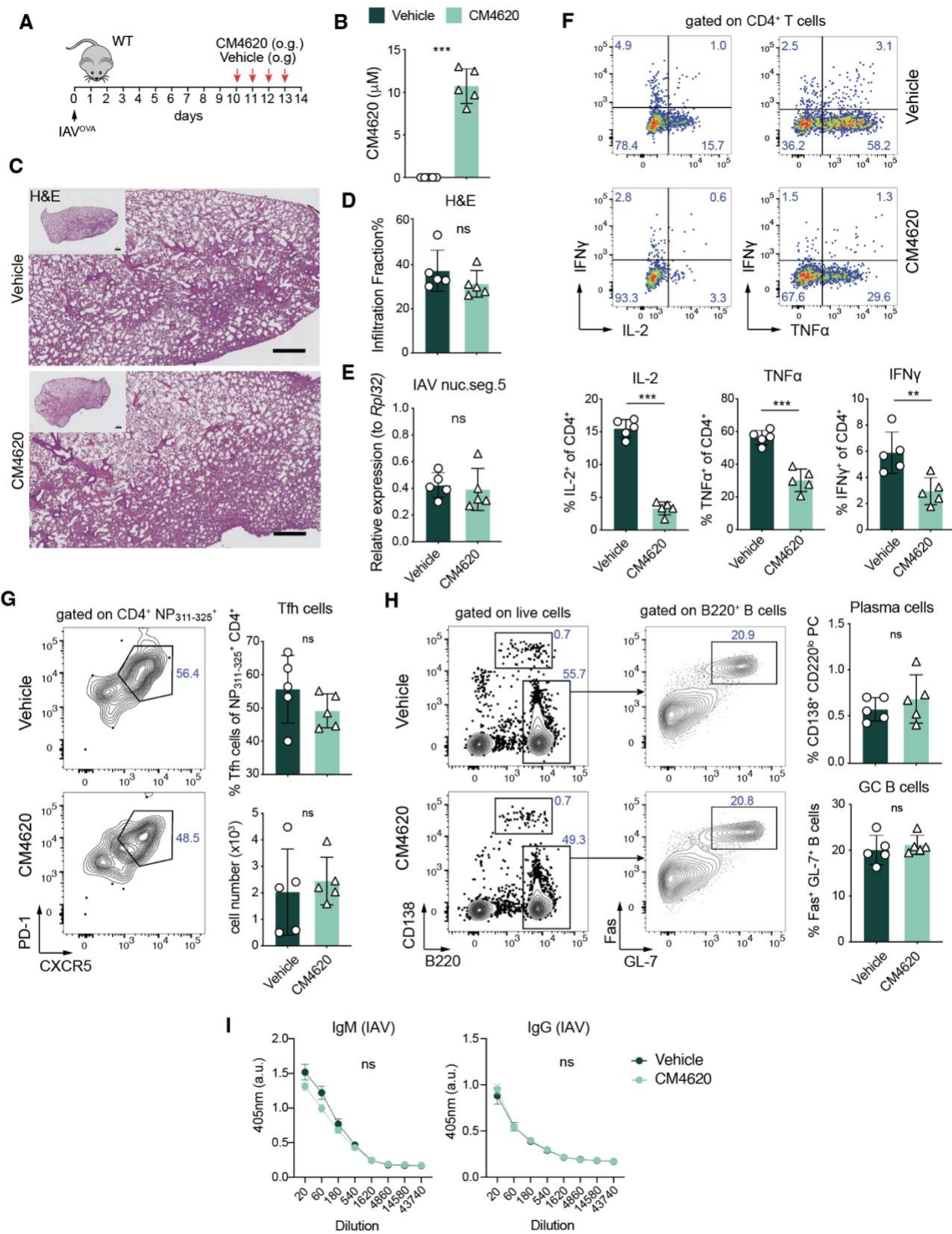


Supplementary Figure 8. ORAI1 is required for cytokine production by Th1 and Th2 cells. A, Representative flow cytometry plots and frequencies of IFN γ , IL-10, TNF α and IL-2 producing CD4⁺ Th1 and Th2 cells *in vitro* that were analyzed after 5 days of polarization *in vitro* and stimulation with PMA/ionomycin for 4h. **B,** Representative flow cytometry plots of TNF α and IFN γ producing CD4⁺ T cells

from WT and *Orai1^{fl/fl}Cd4Cre* mice that were differentiated into Th1 and Th2 cells *in vitro* for 3 days. The isotype control for cytokine antibodies was rat IgG_{1,κ} conjugated with APC or PE. FMO was determined by staining with anti-CD4 (APC-Cy7), and LIVE/DEAD™ Fixable Blue Dead Cell Stain without either anti-TNF-α or anti-IFN-γ. **C**, GATA3 protein levels in CD4⁺ T cells from WT and *Orai1^{fl/fl}Cd4Cre* mice that were differentiated into Th2 cells for 5 days *in vitro*. The isotype control for anti-GATA3 antibody is rat IgG_{2b,κ} conjugated with eF660. FMO was determined by staining with anti-CD4 (APC-Cy7) antibody without anti-GATA3 (eF660). Data are the mean ± SEM of 3-7 mice per genotype from at least 3 independent experiments. Statistical analysis by unpaired Student's t-test with the following significance levels: *** $p < 0.001$; ** $p < 0.01$; * $p < 0.05$.



Supplementary Figure 9. ORAI1 is required for the maintenance of GATA3, IRF4 and BATF expression by Th2 cells *in vitro*. **A,B**, Analysis of IRF4 and BATF expression by CD4⁺ T cells of WT and *Orai1^{fl/fl}Cd4Cre* mice that were polarized into Th2 cells (IL-4, anti-IFN γ) *in vitro* and analyzed at days 3 and 5 in culture. **A**, Representative histogram plots and quantification of IRF4 protein levels (MFI) analyzed by flow cytometry (left) and *Irf4* mRNA expression analyzed by qRT-PCR (right), normalized to RPL32 and WT. **B**, *Batf* mRNA expression analyzed by qRT-PCR, normalized to *Rpl32* house keeping gene and WT T cells. Data in A and B are the mean \pm SEM of 3-4 mice per genotype from at least 3 representative experiments. Statistical analysis by 2-way ANOVA with Sidak's multiple comparison (mRNA in A,B) and paired Student's t-test (protein in A). *** $p < 0.001$ ** $p < 0.01$ * $p < 0.05$. **C**, Proposed model of the effects of ORAI1 and SOCE on Th2 cell differentiation and maintenance. Cytokines, transcription factors and pathways shown in red are decreased in the absence of ORAI1. Dashed red boxes indicate molecules whose function is presumed to be impaired but that were not measured directly. The red triangle and dashed line downstream of Ca²⁺ indicate that BATF and IRF4 expression requires SOCE as shown in (9) but is not impaired in the absence of ORAI1 and partial reduction of SOCE during initial T cell activation.



Supplementary Figure 10. Pharmacological CRAC channel inhibition does not compromise adaptive immunity to influenza A virus infection. **A**, Protocol used for infection of wildtype (WT) C57BL/6J mice with the x31 (H3N2) strain of influenza A virus (IAV). Mice were treated with 25 mg per kg

bodyweight of CM4620 or vehicle alone by oral gavage (o.g.) on four consecutive days and analyzed 14 days p.i. **B**, Concentrations of CM4620 in the serum of mice measured by LC-MS. **C**, Representative H&E stains of lung sections of mice. Scale bars represents 500 μm . **D**, Percentage of lung area with leukocyte infiltration based on H&E stains in (C). **E**, Virus burdens in the lungs of mice treated with CM4620 or vehicle at day 14 p.i. measured by qRT-PCR of nuclear segment 5 of IAV. **F**, Frequencies of CD4⁺ T cells producing IL-2, IFN- γ and TNF- α . T cells were isolated from the lungs of mice at day 14 p.i. and restimulated *in vitro* with PMA / ionomycin for 4h and analyzed by flow cytometry. **G**, Frequencies and total numbers of PD-1⁺ CXCR5⁺ T follicular helper (Tfh) cells specific for nuclear protein (NP) antigen of IAV that were isolated from the mediastinal lymph nodes (mLNs) of mice 14 days p.i. **H**, Frequencies of B220⁺ GL-7⁺ Fas⁺ germinal center (GC) B cells and B220^{int} CD138⁺ plasma cells (PC) in the mLNs of mice. **I**, Serum levels of IAV-specific IgM and IgG antibodies at day 14 p.i. measured by ELISA. Data in D-I are the mean \pm SEM of 5 mice per cohort from 2 independent experiments. Statistical analysis by unpaired Student's t-test: *** $p < 0.001$; ** $p < 0.01$; * $p < 0.05$. ns, not significant.

SUPPLEMENTARY TABLES

Supplementary Table 1. Primers for realtime PCR.

Gene	Forward primer	Reverse primer
<i>Il4</i>	CGAGCTCACTCTCTGTGGTG	TGAACGAGGTCACAGGAGAA
<i>Il13</i>	CACACTCCATACCATGCTGC	TGTGTCTCTCCCTCTGACCC
<i>Il5</i>	CCCACGGACAGTTTGATTCT	GCAATGAGACGATGAGGCTT
<i>Il6</i>	TAGTCCTTCCTACCCCAATTTCC	TTGGTCCTTAGCCACTCCTTC
<i>Tnfa</i>	AGGGTCTGGGCCATAGAACT	CCACCACGCTCTTCTGTCTAC
<i>Il33</i>	ACTATGAGTCTCCCTGTCCTG	ACG TCA CCCCTTTGA AGC
<i>Mcp1 (Ccl2)</i>	TGATCCCAATGAGTAGGCTGGAG	ATGTCTGGACCCATTCTTCTTG
<i>Mcp3 (Ccl7)</i>	CCTGGGAAGCTGTTATCTTCAA	TGGAGTTGGGGTTTTTCATGTC
<i>Eotaxin1 (Ccl11)</i>	GCGCTTCTATTCTGCTGCTCACGG	GTGGCATCCTGGACCCACTTCTTC
<i>Eotaxin2 (Ccl24)</i>	GCCTCCTTCTCCTGGTAGCCTGC	ATGGCCCTTCTTGGTGATGAAGAT
<i>Rantes (Ccl5)</i>	ATGAAGATCTCTGCAGCTGCCCT	ACTTCTTCTCTGGGTTGGCACACA
<i>M2 protein (Ion channel)</i>	AAGACCAATCCTGTACCTCTGA	CAAAGCGTCTACGCTGCAGTCC
<i>M1 protein (Matrix)</i>	CCGAGATCGCACAGAGACTTGAAGAT	GGCAAGTGCACCAGCAGAATAACT
<i>Segment 5 (nucleoprotein)</i>	GCACGGTCAGCACTCATTCTGAG	GACCAAATGAAAACCCAGCTCA
<i>Segment 7 (pre-mRNA M1 and M2)</i>	AGCCAAGTGTACAGCCTAATC	CTTCAAATGCGGCAGAATGG
<i>Segment 7 (pre-mRNA M1 and M2)</i>	CAGATGGAGACTGATGGAGAAC	GGTGACATTTGGATGTAGAATC
<i>Gata3</i>	AGGATGTCCCTGCTCTCCTT	GCCTGCGGACTCTACCATAA
<i>Irf4</i>	GCAATGGGAACTCCGACAGT	CAGCGTCCTCCTCACGATTGT
<i>Batf</i>	GCGTTCTGTTTCTCCAGGTC	AGAGAGAAGAATCGCATCGC
<i>Ccna2</i>	GTGGTGATTCAAACTGCCA	AGAGTGTGAAGATGCCCTGG
<i>Mcm6</i>	TGCACGAGCCTCTTCCCTACT	TCCCGCATGTCCATCTTATCA

<i>Bub1</i>	AGAATGCTCTGTCAGCTCATCT	TGTCTTCACTAACCCACTGCT
<i>Cdk1</i>	AGAAGGTACTTACGGTGTGGT	GAGAGATTTCCCGAATTGCAGT

Supplementary Table 2. Antibodies for flow cytometry.

Antigen	Manufacturer	Clone	Conjugation
B220	eBioscience	RA3-6B2	FITC
B220	eBioscience	RA3-6B2	PB
B220	Biologend	RA3-6B2	BV510
BCL6	eBioscience	BCL-DWN	PE
BrdU	eBioscience	BU20A	FITC
CCR7	eBioscience	4B12	APC
CD11b	eBioscience	M1/70	PE-Cy7
CD11c	Biologend	N418	FITC
CD16/32 (Fc block)	eBioscience	93	Non-conjugated
CD16/32 (Fc block)	BioXcell	2.4G2	Non-conjugated
CD38	eBioscience	90	APC
CD38	Biologend	T10	PE-Cy7
CD4	eBioscience	GK1.5	PB
CD4	Biologend	GK1.5	APC-Cy7
CD4	eBioscience	GK1.5	PE-Cy7
CD44	eBioscience	IM7	FITC
CD44	eBioscience	IM7	PB
CD44	eBioscience	IM7	PerCP-Cy5.5
CD44	eBioscience	IM7	PE-Cy7
CD62L	Biologend	Mel-14	PerCP-Cy5.5
CD69	eBioscience	H1.2F3	FITC
CD69	eBioscience	H1.2F3	PE
CD8	eBioscience	53-6.7	PB
CD8	eBioscience	53-6.7	APC
CD8	eBioscience	53.6-7	PE
CD95(Fas)	BD Bioscience	Jo2	BV421
CD138	Biologend	281-2	PE
CXCR5	eBioscience	SPRCL5	PerCP-eFluor™ 710
CXCR5	Biologend	L138D7	BV421
FOXP3	eBioscience	FJK-16s	PE
GATA3	eBioscience	TWAJ	eFluor® 660

GL-7	Biolegend	GL7	Alexa-Fluor647
GL-7	Biolegend	GL7	FITC
GR-1 (Ly6G)	Biolegend	1A8	Alexa-Fluor647
IFN- γ	eBioscience	XMG1.2	APC
IFN- γ	Biolegend	XMG1.2	PE
IFN- γ	eBioscience	XMG1.2	PE
IFN- γ	Biolegend	XMG1.2	BV421
IL-10	Biolegend	JES5-16E3	FITC
IL-13	eBioscience	eBio13A	Alexa-Fluor488
IL-17A	Biolegend	TC11-18H10.1	FITC
IL-17A	eBioscience	eBio17B7	PerCP-Cy5.5
IL-2	eBioscience	JES6-5H4	FITC
IL-2	Biolegend	JES6-5H4	PE
IL-21	eBioscience	mhalx21	PE
IL-4	eBioscience	11B11	PE
IL-5	Biolegend	TRFK5	PE
IRF4	eBioscience	3E4	eFluor® 660
MHC II	eBioscience	25UG	PB
PD-1	Biolegend	29F.1A12	PE-Cy7
PD-1	eBioscience	J43	APC
Siglec-F	BD Biosciences	E50-2440	PE
T-bet	eBioscience	eBio4B10	PerCP-Cy5.5
T-bet	eBioscience	eBio4B10	PE
TNF- α	eBioscience	MP6-XT22	APC
Rat IgG1, κ Isotype Ctrl (for IL-13)	eBioscience	eBRG1	Alexa-Fluor488
Rat IgG1, κ Isotype Ctrl (for IL-4)	eBioscience	eBRG1	PE
Rat IgG1, κ Isotype Ctrl (for TNF- α)	eBioscience	eBRG1	APC
Rat IgG1, κ Isotype Ctrl (for IFN- γ)	Biolegend	RTK2071	PE
Rat IgG2b, κ Isotype Control (for GATA3)	eBioscience	eB149/10H5	eFluor 660
ORAI1 (custom-made)	Yenzym Antibodies	Polyclonal (YZ6856)	Non-conjugated
Normal rabbit IgG	Cell Signaling	Polyclonal (2729)	Non-conjugated
Goat anti rabbit IgG	Thermo Fisher	Polyclonal (A21244)	Alexa-Fluor647

Supplementary Table 3. MHC class II tetramers for flow cytometry.

Tetramer	Source	Model	Conjugation
I-A(b)AQVYSLIRPNENPAHK (NP311-25)	NIH Tetramer Core Facility	IVA	PE
I-A(b)AQVYSLIRPNENPAHK (NP311-25)	NIH Tetramer Core Facility	IVA	Alexa-Fluor647
I-A(b) / CQIYPPNVNKI (Derp1)	NIH Tetramer Core Facility	HDM	APC
I-A(b) / CQIYPPNVNKI (Derp1)	NIH Tetramer Core Facility	HDM	PE